Calculation of Propagation Constants and Cutoff Frequencies of Radially Inhomogeneous Optical Fibers

CHING-CHUAN SU AND CHUN HSIUNG CHEN

Abstract —**Based on the finite-difference technique, an efficient numerical method that can treat both the propagation constants and cutoff frequencies of optical fibers with arbitrary permittivity profiles is developed in the rigorous vector form. Such a propagation problem is formulated in transverse fields so that the proposed method does not suffer from spurious modes. The associated boundary conditions including those at cutoff are derived in a novel way. Thereafter, numerical results of the cutoff frequency and propagation constant of a fiber with the parabolic profile are presented.**

I. Introduction

TO SOLVE THE propagation constants of guided modes of optical fibers with arbitrary permittivity profiles in the rigorous vector form, several numerical methods have been developed. They include the stair-case approximation [1], [2], direct numerical integration of four coupled first-order differential equations [3]–[6], and the finite-element method [7]. In the stair-case approximation, the radially inhomogeneous fiber is divided into and is thus approximated by a series of homogeneous regions. In each such region, linear combinations of analytic field distributions (the Bessel or modified Bessel functions) are related to those in the neighboring regions. In the second method, the four tangential components of the electromagnetic fields are related by four coupled first-order differential equations. The propagation problem is solved by matching at the boundary two independent sets of solutions, which in turn are obtained numerically by direct integrations of the four first-order differential equations. The finite-element method in [7] is formulated in the axial fields, which may suffer from spurious modes when the node points are not chosen carefully [8].

Now let us turn to the methods of determining cutoff frequency. As early as 1973, Dil and Blok [3] proposed associated equations, from the four coupled first-order differential equations, for treating the cutoff frequencies of guided modes, but no serious data was presented at that time. Perhaps, the first detailed evaluation of cutoff frequencies in the vector form is due to Bianciardi and Rizzoli [1], who have developed a method based on the stair-case approximation for dealing with the cutoff frequency as well as propagation constant.

Manuscript received July 16, 1985; revised October 28, 1985.

C-C. Su is with the Department of Electrical Engineering, National Tsing Hua University, Hsinchu, Taiwan.

C. H. Chen is with the Department of Electrical Engineering, National Taiwan University, Taipei, Taiwan.

IEEE Log Number 8406850.

In this investigation, from the rigorous vectorial wave equations, we present an efficient finite-difference method in the $H_\phi - H_r$ formulation, which does not suffer from spurious modes and can handle both the propagation constants and cutoff frequencies of optical fibers with arbitrary permittivity profiles. In Section II, two coupled second-order differential equations in H_ϕ and H_r are formulated. Thereafter, the associated boundary conditions are derived, including those at cutoff. The calculated results for the parabolic profile are presented in Section IV.

II. Formulation

Consider an isotropic, rotationally symmetric optical fiber of which the relative permittivity profile, in general, can be expressed as

$$\begin{aligned} \epsilon(R) &= \epsilon_1 + (\epsilon_2 - \epsilon_1)P(R), & R \leqslant 1 \\ &= \epsilon_1, & R > 1. \end{aligned} \tag{1}$$

Here, $R = r/a$, r is the radial variable in cylindrical coordinates, a is the core radius of the fiber, and $P(R)$ is an arbitrary function whose value never exceeds unity such that the relative permittivity never exceeds ϵ_2 ($\epsilon_2 > \epsilon_1$). Along such a fiber, a time-harmonic electromagnetic wave of anular frequency ω propagates with fixed variations with respect to the axial (z) and the azimuthal (ϕ) directions as $\exp(-jm\phi - j\beta z)$, where the azimuthal mode number m is an integer. From Maxwell's equations, one obtaines

$$k_0^2\epsilon(R)\bar{H} + \nabla^2\bar{H} + \frac{\nabla\epsilon(R)}{\epsilon(R)} \times \nabla \times \bar{H} = 0. \tag{2}$$

From such a relation, the propagation problem of the radially inhomogeneous fiber can be described in terms of the transverse magnetic fields, H_ϕ and H_r, as in the following two coupled second-order differential equations:

$$\begin{aligned} &H_\phi''(R) + \frac{1}{R}H_\phi'(R) \\ &\quad + \left[a^2\left(k_0^2\epsilon(R) - \beta^2\right) - \frac{1}{R^2} - \frac{m^2}{R^2}\right]H_\phi(R) \\ &\quad - \frac{2m}{R^2}H_r(R) - \frac{\epsilon'(R)}{\epsilon(R)} \\ &\quad \cdot \left[H_\phi'(R) + \frac{1}{R}H_\phi(R) + \frac{m}{R}H_r(R)\right] = 0 \end{aligned} \tag{3a}$$

and

$$H_r''(R)+\frac{1}{R}H_r'(R)+\left[a^2\left(k_0^2\epsilon(R)-\beta^2\right)-\frac{1}{R^2}-\frac{m^2}{R^2}\right]H_r(R)-\frac{2m}{R^2}H_\phi(R)=0 \tag{3b}$$

where k_0 is the free-space propagation constant and the prime denotes differentiation with respect to R. In writing (3) and throughout this investigation, a prue imaginary number j before H_r is omitted for compactness in notation. Once H_ϕ and H_r are solved, the axial fields, E_z and H_z, can be obtained from the relations of $\nabla\cdot\bar{H}=0$ and $j\omega\epsilon_0\epsilon(R)\bar{E}=\nabla\times\bar{H}$, respectively. Explicitly

$$-\tilde{H}_z(R)=H_r'(R)+\frac{1}{R}H_r(R)+\frac{m}{R}H_\phi(R) \tag{4a}$$

and

$$\tilde{E}_z(R)=\left[H_\phi'(R)+\frac{1}{R}H_\phi(R)+\frac{m}{R}H_r(R)\right]/\epsilon(R) \tag{4b}$$

where $\tilde{E}_z(R)=j\omega\epsilon_0 aE_z(R)$ and $\tilde{H}_z(R)=\beta aH_z(R)$.

To solve (3), we need two boundary conditions at $R=0$ and the other two at the core-cladding interface. From (4), it is noted that, for E_z and H_z to remain finite at $R=0$, it requires that

$$\left.\begin{aligned}H_\phi(0)&=0\\H_r(0)&=0\end{aligned}\right\}\quad\text{for } m\neq 1 \tag{5a, 5b}$$

and that

$$H_\phi(0)=-H_r(0)\qquad\text{for } m=1. \tag{6}$$

Using (6), one can find that, for the left-hand sides of (3a) and (3b) to still remain finite at $R=0$, it requires that

$$\left.\begin{aligned}H_\phi'(0)&=0\\H_r'(0)&=0\end{aligned}\right\}\quad\text{for } m=1. \tag{5c, 5d}$$

The other two boundary conditions at the core-cladding interface ($R=1$) are derived as follows. As shown in [9], H_ϕ and H_r can be expressed in terms of E_z and H_z. For the cladding region ($R>1$), the expressions read as

$$\begin{bmatrix}H_\phi(R)\\H_r(R)\end{bmatrix}=\frac{1}{w^2}\begin{bmatrix}\epsilon_1 wK_m'(wR)/K_m(wR) & m/R\\ -\epsilon_1 m/R & -wK_m'(wR)/K_m(wR)\end{bmatrix}\cdot\begin{bmatrix}\tilde{E}_z(R)\\\tilde{H}_z(R)\end{bmatrix} \tag{7}$$

where $w=a(\beta^2-k_0^2\epsilon_1)^{1/2}$, $K_m(wR)$ is the mth-order modified Bessel function of the second kind, and $K_m'(wR)=dK_m(wR)/d(wR)$. The axial component fields in (7), in turn, can be expressed in terms of H_ϕ and H_r as stated by (4). Thus, (5) and (7) constitute the boundary conditions of the propagation problem in the $H_\phi-H_r$ formulation.

It is noted that (7) requires special consideration at cutoff ($w\to 0$) since the common denominator w^2 vanishes in such a situation. Following a similar procedure as in [10], such a singularity can be removed by noting the behavior of the modified Bessel functions with vanishing arguments, as follows.

As w approaches zero, K_0'/K_0w becomes infinite. Thus, for $H_\phi(1)$ and $H_r(1)$ in (7) to remain finite, it requires that

$$\left.\begin{aligned}\tilde{E}_z(1)&=0\\\tilde{H}_z(1)&=0\end{aligned}\right\}\quad\text{for } m=0. \tag{8a, 8b}$$

For $m>0$, wK_m'/K_m approaches a quantity of $[-m/R-w^2Q_mR]$, where

$$Q_1=-\ln(1.781wR/2)$$

and

$$Q_m=1/2(m-1)\qquad\text{for } m>1.$$

Again, for $H_\phi(1)$ and $H_r(1)$ in (7) to remain finite, it requires that, to the order of w^2

$$\tilde{H}_z(1)=\epsilon_1\tilde{E}_z(1)+w^2f \tag{9}$$

where f is an unknown quantity. From such a relation, one can substitute $\tilde{E}_z$ for $\tilde{H}_z$ in (7). Thereby, one obtains

$$\begin{bmatrix}H_\phi(1)\\H_r(1)\end{bmatrix}=\begin{bmatrix}-\epsilon_1Q_m & m\\ \epsilon_1Q_m & m\end{bmatrix}\begin{bmatrix}\tilde{E}_z(1)\\f\end{bmatrix} \tag{10}$$

and then

$$H_\phi(1)-H_r(1)=-2\epsilon_1Q_m\tilde{E}_z(1). \tag{11a}$$

Letting $w=0$ in (9), one obtains the other boundary condition at cutoff as

$$\tilde{H}_z(1)=\epsilon_1\tilde{E}_z(1). \tag{11b}$$

It is noted that the newly introduced unknown f has been cancelled in (11a). Since Q_1 becomes infinite, the boundary conditions at cutoff, (11a) and (11b), for the case of $m=1$ reduce to those for $m=0$, (8a) and (8b). When $\tilde{E}_z(1)$ and $\tilde{H}_z(1)$ in the boundary conditions (7), (8), or (11) are expressed in terms of H_ϕ and H_r (from (4)), one arrives at the desired boundary conditions in the present $H_\phi-H_r$ formulation.

It is of interest to consider the special case of step profile ($P(R)=1$). For such a case, $E_z(R)$ and $H_z(R)$ satisfy the same differential equation in the homogeneous core region and the same boundary condition at $R=0$. Consequently, they are related linearly as $\tilde{H}_z(R)=c\tilde{E}_z(R)\alpha J_m(uR)$ (for $0\leqslant R\leqslant 1$), where c is a constant, J_m is the mth-order Bessel function of the first kind, and $u=a(k_0^2\epsilon_2-\beta^2)^{1/2}$. For (11b) to be satisfied at cutoff, one can conclude that $c=\epsilon_1$, otherwise $\tilde{E}_z(1)=\tilde{H}_z(1)=0$. In the former case, $\tilde{H}_z(R)=\epsilon_1\tilde{E}_z(R)$, when $H_\phi(1)$ and $H_r(1)$ in (11a) are expressed in $\tilde{E}_z(1)$ and $\tilde{H}_z(1)$ using a similar form of (7) for the core region, (11a) reduces to the cutoff equation derived by Schelkunoff [11] for the HE modes with $m\geqslant 2$. The latter case, or stated by (8), is just the cutoff equation of the EH modes obtained by Aebel [12].

It is of convenience to introduce normalized frequency V and normalized propagation constant B, where

$$V = k_0 a(\epsilon_2 - \epsilon_1)^{1/2}$$

and

$$B = \left[(\beta/k_0)^2 - \epsilon_1\right]/(\epsilon_2 - \epsilon_1).$$

If such normalized quantities are substituted in (3) and in the associated boundary conditions, it can be shown that (except the TE modes for which $m = 0$ and $H_\phi = 0$) the relation between B and V of guided modes are determined by the permittivity ratio $\epsilon_r (= \epsilon_2/\epsilon_1)$, not necessarily by the respective values of ϵ_2 and ϵ_1. As to the TE modes, the situation relaxes further; that is, the relation between B and V is determined by the profile $P(R)$ only and is independent of ϵ_2 and ϵ_1.

III. Numerical Procedure and Efficiency

To solve the two coupled second-order differential equations (3) together with the associated boundary conditions, we discretize equally the interval $(0 \leqslant R \leqslant 1)$ into N node points R_i $(i = 1, 2, \cdots, N)$ and calculate the corresponding fields at such points. Applying the central finite-difference formulas to (3) and to the associated boundary conditions (except for (5c) and (5d), where a forward finite difference is used), and employing a similar (generalized in a bivariable form) approach as in [13], we arrive at $2N$ simultaneous linear equations.

$$A\Psi = 0 \tag{12}$$

where A is a $2N \times 2N$ band matrix with a bandwidth of 5 and

$$\Psi = \left[H_\phi(R_1) H_r(R_1) \cdots H_\phi(R_N) H_r(R_N)\right]^T.$$

To obtain the cutoff frequency of each guided mode, we set $\beta^2 = k_0^2 \epsilon_1$ $(B = 0)$ and search the value of normalized frequency V such that the determinant of A becomes vanishing. The dispersion curves of guided modes are constructed by fixing V (or B) and then searching the value of B (or V) which renders $\det A$ vanishing.

In the cases of $m \neq 0$, the computation effort for each trial set of B and V of the proposed method lies mainly in the Gauss elimination of the band matrix A, which takes $12N$ multiplications. The required core memory is about $20N$ locations of storage. In the case of $m = 0$, $H_\phi(R)$ and $H_r(R)$ are uncoupled in the formulation and the computation effort can be reduced accordingly.

IV. Results

The proposed method can treat any kind of permittivity profile. In this investigation, we consider the parabolic profile $(P(R) = 1 - R^2)$, for which the present results can be compared with other works. The number of node points N chosen in this section is 100, except when stated otherwise. The notation TE (TM) corresponds to the mode of $m = 0$ and $H_\phi(H_r) = 0$. In the cases of $m > 0$, the modes are hybrid. The notation HE (EH) corresponds to the mode for which the maxima of the corresponding $\tilde{E}_z(R)$ and $\tilde{H}_z(R)$ are of the same (opposite) sign.

TABLE I
Normalized Cutoff Frequencies of Optical Fibers with the Parabolic Profile

	ϵ_r = 1.0404				ϵ_r = 2.25		
Mode	I.	II.	III.	IV.	V.	VI.	VII.
HE_{11}	0.00	0.00	0.00	0.00	0.00	0.00	0.00
TM_{01}	3.501	3.502	3.502	3.502	3.230	3.230	3.230
TE_{01}	3.517	3.518	3.518	3.518	3.518	3.518	3.518
HE_{21}	3.532	3.532	3.532	3.533	3.870	3.879	3.882
HE_{12}	5.061	5.070	5.066	5.065	5.005	5.001	5.001
EH_{11}	5.733	5.732	5.733	5.733	5.570	5.572	5.572
HE_{31}	5.760	5.760	5.761	5.761	6.149	6.157	6.160
TM_{02}	7.438	7.435	7.440	7.441	7.231	7.238	7.238
TE_{02}	7.450	7.446	7.451	7.451	7.446	7.451	7.451
HE_{22}	7.455	7.451	7.456	7.457	7.542	7.552	7.555
EH_{21}	7.835	7.834	7.835	7.836	7.649	7.652	7.653
HE_{41}	7.865	7.864	7.866	7.866	8.273	8.281	8.283
HE_{13}	9.144	9.156	9.156	9.156	9.093	9.094	9.094
EH_{12}	9.636	9.619	9.637	9.638	9.500	9.518	9.518
HE_{32}	9.652	9.644	9.653	9.654	9.855	9.871	9.875
EH_{31}	9.890	9.889	9.891	9.891	9.641	9.644	9.645
HE_{51}	9.923	9.920	9.923	9.923	10.339	10.346	10.348

The data in column I are taken from [1]; those in columns II and V (III and VI) are made here with $N = 30$ (100).

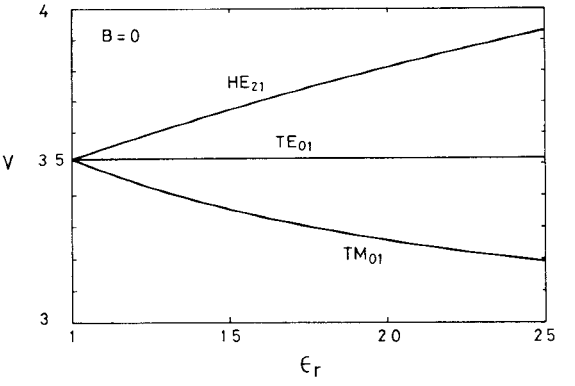

Fig. 1. Cutoff frequencies of three lower modes as functions of ϵ_r.

The calculated cutoff frequencies of the first 17 modes of the parabolic profile are presented in Table I. The data presented in volumns IV and VII of Table I are believed to be exact, since no deviations in the third decimal digit were observed when larger values of N were used. All the data in column IV ($\epsilon_r = 1.0404$) are achieved with $N = 300$; most of the data in column VII ($\epsilon_r = 2.25$) are achieved with $N = 1000$. For comparison, we also list the results from Bianciardi and Rizzoli [1] in column I. It is seen that their results show some discrepancies from those in column IV, especially for the HE_{13} mode.

The variations of the cutoff frequencies of the TE_{01}, TM_{01}, and HE_{21} modes as the permittivity ratio increases are shown in Fig. 1. It is seen that as ϵ_r approaches unity, the above three modes become degenerate. As ϵ_r increases, the cutoff frequency of the HE_{21} modes increases, while

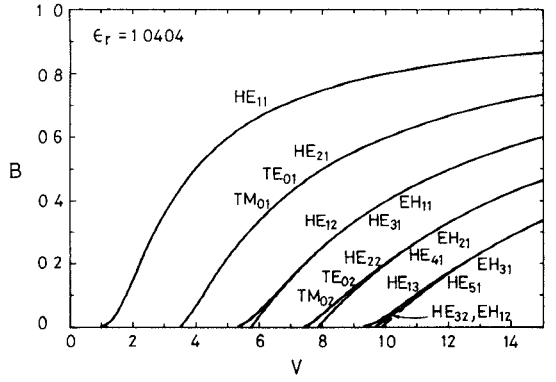

Fig. 2. Dispersion curves of the first 17 modes of the parabolic profile with $\epsilon_r = 1.0404$.

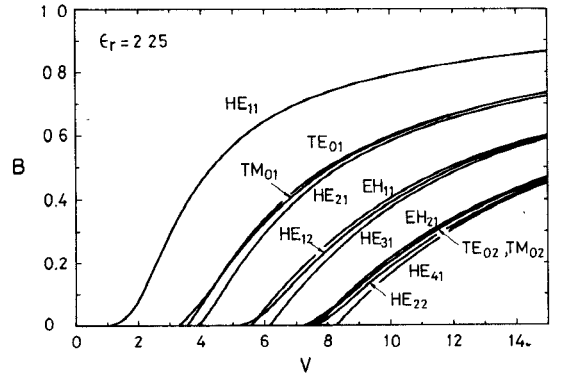

Fig. 3. Dispersion curves of the first 12 modes of the parabolic profile with $\epsilon_r = 2.25$.

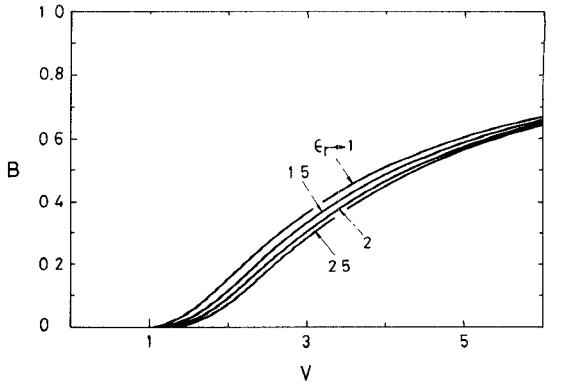

Fig. 4. Dispersion curve of the fundamental (HE_{11}) mode with ϵ_r as a parameter.

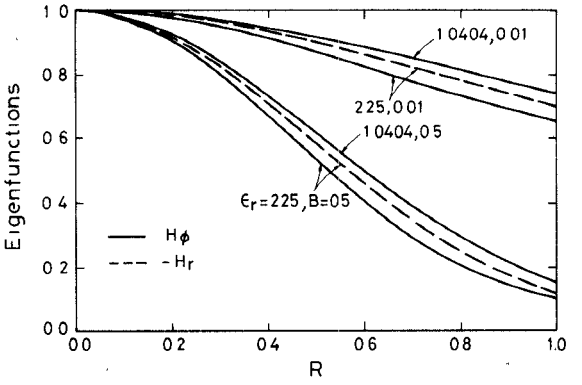

Fig. 5. Field distributions of the fundamental (HE_{11}) mode (in relative magnitude) with the normalized propagation constant and the permittivity ratio as parameters. The discrepancies between the curves of H_ϕ and H_r are too small to be shown for the cases of $\epsilon_r = 1.0404$.

that of the TM_{01} mode decreases. As noted in Section II, it is seen that the cutoff frequency of the TE_{01} mode is independent of the permittivity ratio. Since the vectorial solution becomes the scalar one when ϵ_r approaches unity, the vectorial and the scalar results of the TE modes become identical, regardless of the permittivity ratio. Exact solutions of cutoff frequencies of the parabolic profile in the scalar form can be obtained analytically via the Kummer functions and have been calculated by Lukowski and Kapron [14]. From them, the exact values of normalized cutoff frequencies of the TE_{01} and the TE_{02} modes are given as 3.518 and 7.451, respectively, which agree with our presented data.

Dispersion curves of the first 17 guided modes of the parabolic profile with $\epsilon_r = 1.0404$ are shown in Fig. 2. From Fig. 2, it is seen that due to $\epsilon'(R)$ being negligibly small, the $HE_{m+1,l}$ mode and the $EH_{m-1,l}$ mode (or the TM_{0l} and TE_{0l} modes, when $m = 1$) become nearly degenerate. Similar degeneracy also exists in the dispersion curves of the HE_{ml} mode and the $EH_{m,l-1}$ mode in the region of far above cutoff. (Note that the latter near-degeneracy may not hold in other profiles, as shown in Fig. 7.) When the permittivity ratio is increased, two such kinds of near-degeneracy are removed somewhat, as indicated in Fig. 3. To demonstrate the effect of the permittivity ratio on the propagation characteristics, the shifting of the dispersion curve of the fundamental (HE_{11}) mode as ϵ_r is varied is shown in Fig. 4. It is seen that the curve shifts downwards when the permittivity ratio is increased.

The corresponding eigenfunctions (field distributions of guided modes) are illustrated in Figs. 5 and 6. It is seen that for a higher B, the fields are more concentrated in the core region and that the discrepancy between $H_\phi(R)$ and $H_r(R)$ becomes stronger as ϵ_r is increased. It is noted that the HE_{11} modes have the largest fields at the core center, while the EH_{11} modes do not. From such field distributions, the power distributions [2], [5] and group velocities [15] can be deduced.

In an actual fabrication, there may be a central dip in the permittivity profile. To investigate the effect of the dip, we assume the Gaussian dip, namely, $P(R) = 1 - R^2 - G_d \exp[-(R/G_w)^2]$. The corresponding dispersion curves are shown in Fig. 7, from which it is seen that the curves are lower with a larger G_d. It is noted that the dip has weaker effects on the EH_{11} modes and those modes with $m \neq 1$. This fact is accounted for by noting that the field distributions of such modes are smaller at the core center (from Fig. 6 or (5)) where the dip is located. Since the effects of a central dip are different for the HE_{12} and the EH_{11} modes, it is expected that the near-degeneracy between such two modes (in the case of $G_d = 0$) is removed at the presence of a dip, as shown in Fig. 7 and, similarly, in [6].

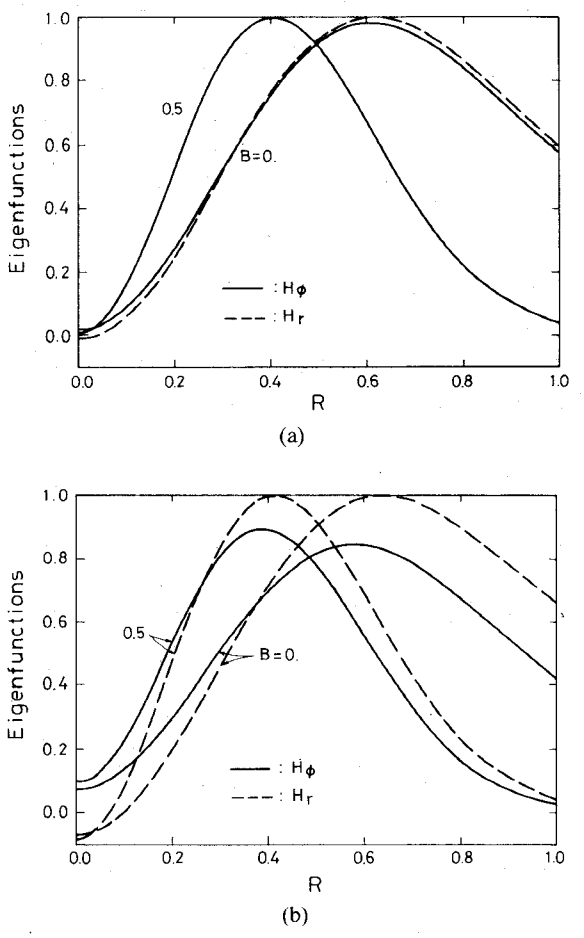

Fig. 6. Field distributions of the EH_{11} mode (in relative magnitude) with the normalized propagation constant as a parameter. (a) $\epsilon_r = 1.0404$. (b) $\epsilon_r = 2.25$. The discrepancy between the curves of H_ϕ and H_r is too small to be shown in (a) for $B = 0.5$.

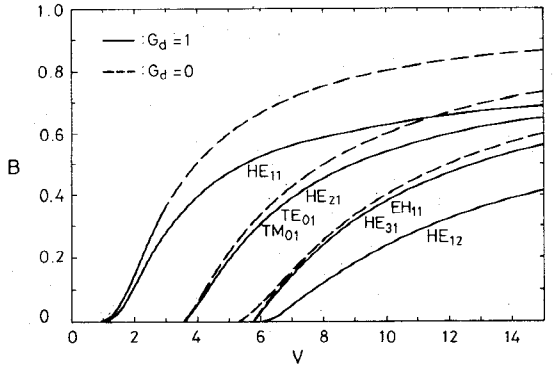

Fig. 7. Dispersion curves of some lower modes of the parabolic profile ($\epsilon_r = 1.0404$) with the Gaussian dip ($G_w = 0.2$).

V. Conclusion

Based on the finite-difference technique, an efficient and rigorous method has been developed which can treat propagation constants as well as cutoff frequencies of optical fibers with arbitrary permittivity profiles. The propagation problem is formulated in transverse fields such that the proposed method does not suffer from spurious modes. Associated boundary conditions are derived, including those at cutoff. Calculated results of the cutoff frequencies and the dispersion curves of optical fibers with the parabolic profile are presented. The effects of the permittivity ratio and the Gaussian dip are also discussed.

References

[1] E. Bianciardi and V. Rizzoli, "Propagation in graded-core fibers: A unified numerical description," *Opt. Quantum Electron.*, vol. 9, pp. 121–133, 1977.

[2] C. Yeh and G. Lindgren, "Computing the propagation characteristics of radially stratified fibers: An efficient method," *Appl. Opt.*, vol. 16, pp. 483–493, Feb. 1977.

[3] J. G. Dil and H. Blok, "Propagation of electromagnetic surface waves in a radially inhomogeneous optical waveguide," *Opto-Electron.*, vol. 5, pp. 415–428, 1973.

[4] G. L. Yip and Y. H. Ahmew, "Propagation characteristics of radially inhomogeneous optical fibre," *Electron. Lett.*, vol. 10, pp. 37–38, Feb. 1974.

[5] G. E. Peterson, A. Carnevale, U. C. Paek, and D. W. Berreman, "An exact numerical solution to Maxwell's equations for lightguides," *Bell Syst. Tech. J.*, vol. 59, pp. 1175–1196, Sept. 1980.

[6] G. L. Yip and H. H. Yao, "Numerical study of radially inhomogeneous optical fibers using a predictor-corrector method," *Appl. Opt.*, vol. 21, pp. 4308–4315, Dec. 1982. (Note the mispagination between pp. 4310 and 4311.)

[7] K. Okamoto and T. Okoshi, "Vectorial wave analysis of inhomogeneous optical fibers using finite element method," *IEEE Trans. Microwave Theory Tech.*, vol. MTT-26, pp. 109–114, Feb. 1978.

[8] C. C. Su, "Origin of spurious modes in the analysis of optical fibre using the finite-element or finite-difference technique," *Electron. Lett.*, vol. 21, pp. 858–860, Sept. 1985.

[9] A. H. Cherin, *An Introduction to Optical Fibers*. New York: McGraw-Hill, 1983, ch. 5.

[10] C. C. Su, "Cutoff frequency of a homogeneous optical fiber with arbitrary cross section," *IEEE Trans. Microwave Theory Tech.*, vol. MTT-33, pp. 1101–1105, Nov. 1985.

[11] S. A. Schelkunoff, *Electromagnetic Waves*. New York: Van Nostrand, 1943, ch. 10.

[12] E. Snitzer, "Cylindrical dielectric waveguide modes," *J. Opt. Soc. Am.*, vol. 51, pp. 491–498, May 1961.

[13] C. F. Gerald and P. O. Wheatley, *Applied Numerical Analysis*, 3rd ed. Reading, MA: Addison-Wesley, 1984, ch. 6, pp. 365–373.

[14] T. I. Lukowski and F. P. Kapron, "Parabolic fiber cutoffs: A comparison of theories," *J. Opt. Soc. Am.*, vol. 67, pp. 1185–1187, Sept. 1977.

[15] K. Morishita, Y. Obata, and N. Kumagai, "An exact analysis of group velocity for propagation modes in optical fibers," *IEEE Trans. Microwave Theory Tech.*, vol. MTT-30, pp. 1821–1826, Nov. 1982.

Ching-Chuan Su was born in Taiwan on October 2, 1955. He received the B.S., M.S., and Ph.D. degrees in electrical engineering from National Taiwan University in 1978, 1980, and 1985, respectively.

From 1980 to 1982, he was employed in an IC company, where he was responsible for the development of several MOS fabrication processes. In 1985, he joined the faculty of National Tsing Hua University, Hsinchu, Taiwan, where he currently serves as an Associate Professor in electrical engineering. His theoretical interests include bistability in nonlinear optics and numerical methods in dielectric waveguide, body scattering, and MOS device simulation.

Chan Hsiung Chen, photograph and biography unavailable at the time of publication.